

## Supplementary Information for

# Lanthanide Chloride Clusters, $\text{Ln}_x\text{Cl}_{3x+1}^-$ , $x=1-6$ : an Ion Mobility and DFT Study of Isomeric Structures and Interconversion Timescales

Yuto Nakajima<sup>1</sup>, Patrick Weis<sup>2</sup>, Florian Weigend<sup>2,3</sup>, Marcel Lukowski<sup>2,3</sup>,  
Fuminori Misaizu<sup>1</sup>, Manfred M. Kappes<sup>2,4</sup>

<sup>1</sup> Graduate School of Science, Department of Chemistry, Tohoku University, Japan

<sup>2</sup> Institute of Physical Chemistry, Karlsruhe Institute of Technology (KIT), Germany

<sup>3</sup> Institute of Quantum Materials and Technologies, Karlsruhe Institute of Technology (KIT), Germany

<sup>4</sup> Institute of Nanotechnology, Karlsruhe Institute of Technology (KIT), Germany

## Table of Contents

1. CCS-calculations, determination of Lennard-Jones parameters for chlorine and lanthanide atoms .....	2
2. Quantum chemical calculations.....	5
Impact of different choices concerning functional, description of relativity and basis sets .....	5
Relative energies and Gibbs free energies of minima .....	9
Reaction pathways and transition states .....	14
Coordinates .....	18

## 1. CCS-calculations, determination of Lennard-Jones parameters for chlorine and lanthanide atoms

In the trajectory calculations implemented in IMoS the ion-buffer gas interaction is modelled (atom-by-atom) with Lennard-Jones-type interactions with element specific parameters. The LJ-parameters  $\epsilon$  and  $\sigma$  are explicitly calibrated against experimental CCS only of the light elements C, H, N, O, and F. For the other elements the (uncalibrated) default values are  $\epsilon=2.6$  meV and  $\sigma=3.5$  Å. With these values we obtain for the lowest energy structures of  $\text{LaCl}_4^-$ ,  $\text{La}_3\text{Cl}_{10}^-$ ,  $\text{La}_4\text{Cl}_{13}^-$  and  $\text{La}_6\text{Cl}_{19}^-$   ${}^{\text{theo}}\text{CCS}_{\text{N}_2}$  that are on average ca. 7% smaller than the experimental values ( ${}^{\text{TW}}\text{CCS}_{\text{N}_2}$ ), therefore a calibration process is needed. First, we keep for both Cl and Ln the parameter  $\epsilon$  at its default value (2.6 meV), and adjust  $\sigma$  to match experiment and calculation. With  $\sigma_{\text{Cl}}=3.85$  Å  $\sigma_{\text{La}}=3.0$  Å (based on the fact that the radius of  $\text{La}^{3+}$  is ca. 0.8 Å smaller than  $\text{Cl}^-$ ) we obtain a close match for  $\text{La}_4\text{Cl}_{13}^-$  ( ${}^{\text{theo}}\text{CCS}_{\text{N}_2}=194.9$  Å $^2$ ,  ${}^{\text{TW}}\text{CCS}_{\text{N}_2}=196.6$  Å $^2$ ), but for  $\text{LaCl}_4^-$  we underestimate the experimental value by ca. 2.2% ( ${}^{\text{theo}}\text{CCS}_{\text{N}_2}=114.3$  Å $^2$ ,  ${}^{\text{TW}}\text{CCS}_{\text{N}_2}=116.8$  Å $^2$ ), while we overestimate it for  $\text{La}_6\text{Cl}_{19}^-$  by 2.3% ( ${}^{\text{theo}}\text{CCS}_{\text{N}_2}=233.9$  Å $^2$ ,  ${}^{\text{TW}}\text{CCS}_{\text{N}_2}=228.7$  Å $^2$ ). As can be seen in **Figure S1**, the best-matching radius for chlorine decreases from  $\sigma_{\text{Cl}} = 3.95$  Å for  $\text{LaCl}_4^-$  to  $\sigma_{\text{Cl}} = 3.75$  Å for  $\text{La}_6\text{Cl}_{19}^-$ . We decided to use 3.85 Å throughout since it minimizes the overall error. Test calculations show that  $\epsilon$  and  $\sigma$  are correlated, i.e. several combinations thereof can be used to reproduce the experimental data (with the problem remaining that the CCS of the  $\text{LaCl}_4^-$  is underestimated and  $\text{La}_6\text{Cl}_{19}^-$  is overestimated). Furthermore,  $\sigma_{\text{La}}$  is ca. 10-fold less sensitive than  $\sigma_{\text{Cl}}$ , increasing it dramatically from 3 Å $^2$  to 3.5 Å $^2$  increases the  ${}^{\text{theo}}\text{CCS}_{\text{N}_2}$  by merely 1% (see also **Figure 6** in the main text). This reflects the smaller number of lanthanide atoms in the  $\text{Ln}_x\text{Cl}_{3x+1}^-$  cluster and the fact that the chlorine atoms are on average closer to the cluster surface, i.e. in closer contact to the collision gas (nitrogen) molecules. As consequence, we use same the Lennard-Jones parameter for all lanthanides ( $\sigma_{\text{Ln}} = 3.0$  Å). Since partial charges localized on each atom are necessary to model the ion-induced dipole and ion-quadrupole interaction in IMoS, we also tested several charge-localization algorithms implemented in TURBOMOLE, specifically ESP-fit, Mulliken and natural bond analysis. While in some cases the charges assigned differ significantly, the calculated CCS show only a very weak dependence on the partial charge distribution. Since ESP-fit is known to show very weak basis set dependence, we use this algorithm. Since the experiments integrate over the isotope distributions, the calculations were performed with average atomic masses. Isotope effects are below 0.1%, i.e. not resolvable in our experiment.

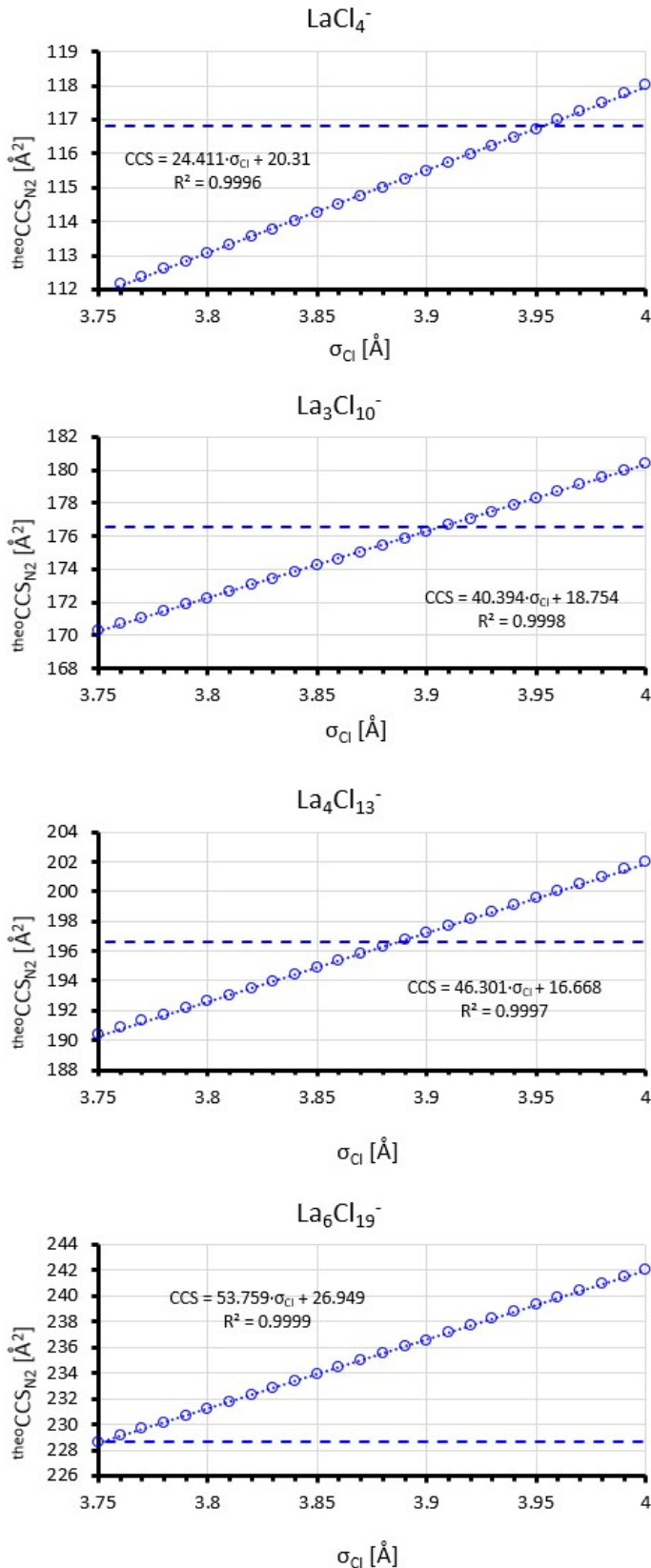


**Figure S1:** Variation of  $\sigma_{\text{Cl}}$  to match the experimental CCS for  $\text{LaCl}_4^-$ ,  $\text{La}_4\text{Cl}_{13}^-$  and  $\text{La}_6\text{Cl}_{19}^-$ . Other parameters are fixed, i.e.  $\sigma_{\text{La}}=3.00$  Å,  $\varepsilon_{\text{Cl}}=\varepsilon_{\text{La}}=2.6$  meV, partial charges by ESP-fit, ion-quadrupole interaction included.

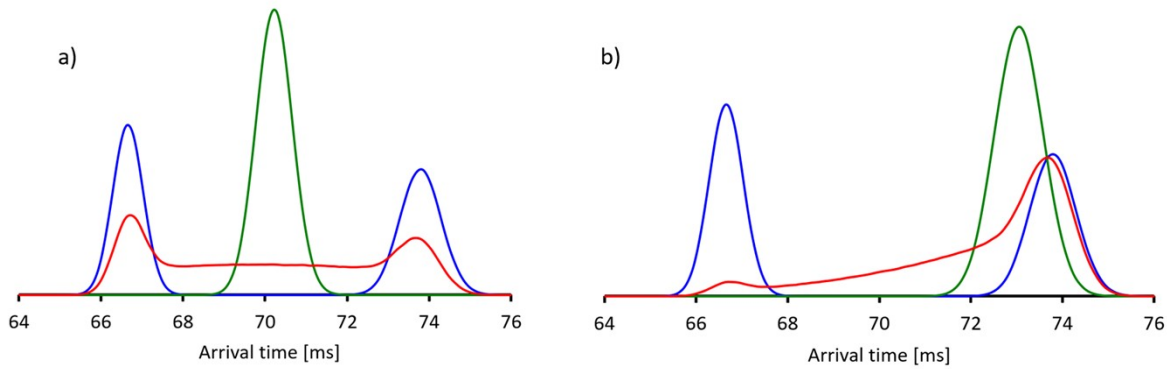


**Figure S2:** Calculated arrival time distributions for two interconverting isomers  $A \rightleftharpoons B$  with interconversion rate constants  $k_{AB}$  and  $k_{BA}$  (based on the formalism developed in ref. 2, main text). The parameters are chosen to closely match the 10-cycle arrival time distributions of  $\text{Ln}_2\text{Cl}_7^-$  (**Figure 2** in main text), i.e. average arrival time of species A is set to 66.5 ms, average arrival time of species B is 73.5 ms (10% difference, centered at 70 ms, which corresponds to the 5% CCS difference of the two isomers due to the square root CCS-arrival time dependence, **Figure 7** in main text). FWHM peak width without interconversion set to 1 ms. Initial intensities  $A_0=B_0$ .

- a) Equal rate constants for interconversion,  $k_{AB} = k_{BA}$ . Blue:  $k_{AB}, k_{BA} = 0$ , i.e. no interconversion during the drift time, green:  $k_{AB}, k_{BA} \rightarrow \infty$ , i.e. many interconversions during the drift time, red: interconversion rate similar to the arrival time.
- b)  $k_{AB} = 10k_{BA}$ . Blue:  $k_{AB}$  and  $k_{BA}$  small, i.e. no interconversion, green:  $k_{AB}, k_{BA} \rightarrow \infty$ , i.e. many interconversions during the drift time, red: interconversion rate similar to the arrival time.

For two species, in the limit of fast interconversions a sharp peak at the weighted average to the individual arrival times is observable, in line with our experimental observation.

## 2. Quantum chemical calculations

The general procedure of finding putatively all low-lying minima and relevant transition states is given in the main text. Here we first focus on the impact of different choices concerning functional, description of relativity and basis sets on the structure parameters of  $\text{LnCl}_4^-$  as well as on the energy surface (minima and transition states) of  $\text{Ln}_2\text{Cl}_7^-$  (**Figures S3-S4, Tables S1-S2**). Next, we list energies and Gibbs free energies, calculated within the harmonic oscillator rigid rotor model, at 0, 300 and 600 K of all relevant minimum structures of  $\text{Ln}_x\text{Cl}_{3x+1}^-$ ,  $\text{Ln}=\text{La-Lu}$ ,  $x=2-6$  (**Tables S3-S7**) with functionals PBE<sup>1</sup> and TPSS<sup>2</sup> employing newly designed and optimized lcecp-1-TZVP bases<sup>3</sup> and display them graphically (**Figures S5-S9**). The bases are listed in the supplementary file `bases.txt`, details of their development will be published elsewhere. The third part is dedicated to transformation pathways (**Figures S10-S13**) and transition state energies and enthalpies (**Tables S8-S9**).

**Impact of different choices concerning functional, description of relativity and basis sets.** DFT structure optimizations in this work were done employing  $f^{n-1}$  large-core effective core-potentials<sup>4</sup> and corresponding recently designed and optimized polarized bases (lcecp-1-XVP, X=SV, T, Q). For the estimation of the reliability concerning structure parameters, different quantum-chemical methods were tested at  $\text{LnCl}_4^-$ . The results are shown in Fig. S3. The impact of the way to describe relativity was investigated for the PBE0 functional<sup>5</sup> by comparing the all-electron relativistic X2C<sup>6</sup> method (x2c-QZVPall bases, in the following termed X2C/QZVPall)<sup>7</sup> and the lcecp-1-QZVP method, thus very close to the DFT basis-set limit. The errors of lcecp-1-TZVP with respect to lcecp-1-QZVP were estimated with the same functional, differences due to the use of different functionals (PBE, TPSS, PBE0) for lcecp-1-TZVP. As evident from Fig. S3, the changes/errors are very similar for all lanthanides and may be summarized as follows:  $d(\text{TZVP})=d(\text{QZVP})-0.3\text{pm}$ ,  $d(\text{PBE})=d(\text{PBE0})+0.8\text{pm}=d(\text{TPSS})-0.8\text{pm}$ ,  $d(\text{ECP})=d(\text{X2C})+2.1\text{pm}$ .

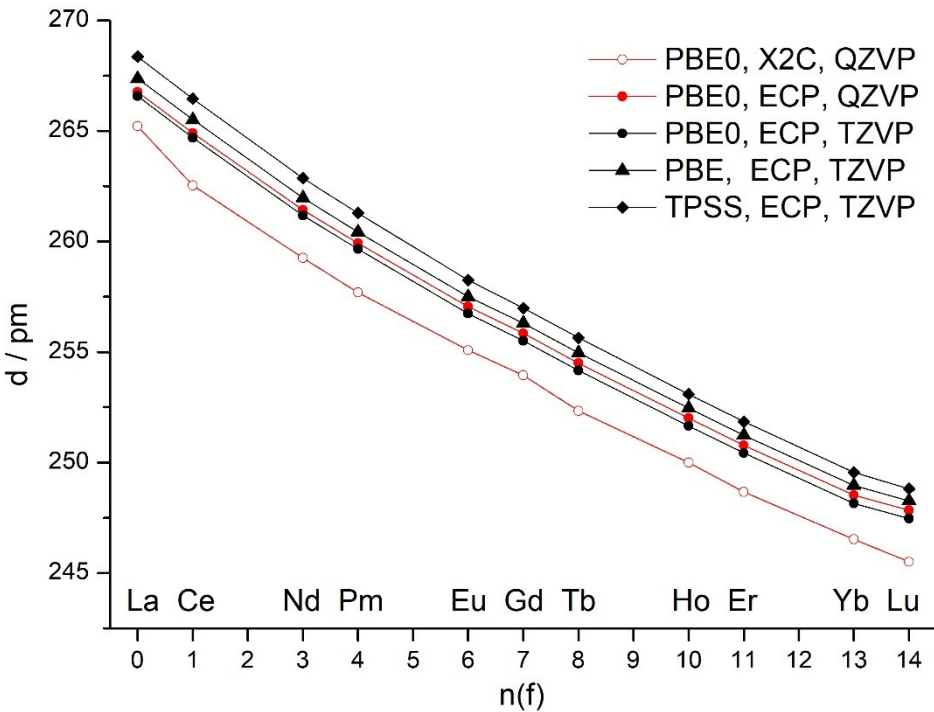


**Figure S3.** Distances obtained for  $\text{LnCl}_4^-$  with various methods for all lanthanides that show either fully, half, or not occupied irreducible representations of the f shell in  $T_d$  symmetry.

The consistency of relative energies of different isomers was assessed at  $\text{Ln}_2\text{Cl}_7^-$  for the same set of methods, **Table S1**, and additionally for PBE/Icecp-1-SVP. For this compound, the two most stable isomers A and B, see **Figure S4**, are of similar energy, and the transition state T between them can be guessed easily. For La, the preference of A over B,  $\Delta_{AB}$ , amounts to 6...12 kJ/mol for all methods (14 kJ/mol for PBE/Icecp-1-SVP and slightly decreases towards Lu, where it amounts to -2...+5 kJ/mol. Functionals TPSS and PBE0 yield very similar values for  $\Delta_{AB}$  throughout, PBE is ca. 5 kJ/mol lower. TZVP and QZVP bases yield almost the same data (differences 0.1...0.4 kJ/mol), errors for the very compact SVP basis are still reasonably small, 2...4 kJ/mol. For ECPs, the decrease of  $\Delta_{AB}$  from La to Lu is strictly monotonic, for all-electron treatments one rather observes steps at the half and at the fully filled f shell: similar numbers clearly above 10 kJ/mol from La to Eu, similar numbers for Gd to Yb around 5 kJ/mol, and 0 kJ/mol for Lu. It is noted that the all-electron relativistic calculation for partially filled f shells does not necessarily lead to more reliable relative energies: depending on details of the f occupation in the initial guess for the wave function, slightly different converged energies and wavefunctions can be obtained, even if Fermi smearing is used; for instance, the energy of B may change by up to ~5 kJ/mol when using the MOs of isomer A instead of Hückel MOs as initial guess. The numbers in **Table S1** are obtained for the first variant of initial MOs throughout. Further, the usage of pure DFT functionals in case of partially filled f shells is sometimes problematic, as they tend to be too high in energy with such functionals, leading sometimes even to incorrect f occupation numbers. This being said, the most reasonable way for economically investigating the energy surface is a pre-scan with a genetic algorithm based on PBE/Icecp-1-SVP level followed by both PBE/Icecp-1-TZVP and TPSS/Icecp-1-TZVP. Finally, it has to be noted that the proven functionals PBE0, PBE or TPSS chosen by

us do not span the full range of obtainable values for  $\Delta_{AB}$ : For  $\text{La}_2\text{Cl}_7^-$  (ECP/TZVP)  $\sim 20$  kJ/mol are obtained with the wB<sup>8</sup> series and also with MP2<sup>9</sup>, and even more than 30 kJ/mol with M06<sup>10</sup> or LHJ14.<sup>11</sup>

**Table S1.** Energies of isomer B in kJ/mol relative to isomer A of  $\text{Ln}_2\text{Cl}_7^-$  for selected lanthanides at different levels of calculation.

	Relativity	Functional	Basis	La	Ce	Nd	Pm	Eu	Gd	Tb	Ho	Yb	Lu
1	ECP	PBE0	QZVP	9.9	9.4	7.9	7.6	6.9	6.6	6.2	5.4	3.7	3.1
2	ECP	PBE0	TZVP	10.3	9.7	8.3	8.0	7.0	6.7	6.4	5.6	3.9	3.3
3	ECP	PBE	TZVP	5.5	4.8	3.3	2.9	1.9	1.6	1.3	0.6	-0.8	-1.5
4	ECP	TPSS	TZVP	9.8	9.3	8.3	8.0	7.3	7.1	6.9	6.5	5.2	4.6
5	As 4, but for the ECP/PBE/TZVP structure			9.7	9.2	8.0	7.7	7.0	6.8	6.6	6.2	4.9	4.3
6	ECP	PBE	SV(P)	14.1	13.4	12.6	11.3	9.1	8.0	7.7	8.4	7.1	5.3
7	X2C	PBE0	QZVP	12.4	15.7	12.4	12.5	15.5	5.6	5.4	2.4	6.1	0.0
8	As 7, but for the ECP/PBE/TZVP structure			11.1	13.5	10.3	10.5	13.2	4.8	4.3	1.7	5.2	-0.5
9	Average of 2,3,4,7			9.5	9.9	8.1	7.9	7.9	5.3	5.0	3.8	3.6	1.6

For a maybe more realistic simulation of the experimental conditions one might also compare the Gibbs free energies, G, of minima and transition states. This is done in **Table S2** for the energy/Gibbs free energy of isomer B and for the transition state (relative to isomer A). For T=0, G is the sum of the electronic energy and the zero-point energy, for finite temperatures further the logarithm of the product of translational, rotational and vibrational sums of states (multiplied by RT) are added. The latter sensitively depends on the vibrational frequencies, which requires tight settings for convergence criteria. Here and in the following, for the structure optimization we chose  $10^{-8} \text{ E}_h$  for the energy and  $10^{-5}$  for the norm of the gradient, the SCF procedure was done with fine grids (gridsize 5)<sup>12</sup> and weight derivatives, and an SCF energy convergence threshold of  $10^{-9} \text{ E}_h$ .

**Table S2.** Electronic energies E of isomer B and the transition state T between isomer A and isomer B of  $\text{Ln}_2\text{Cl}_7^-$  relative to isomer A with PBE/Icecp-1-TZVP and TPSS/Icecp-1-TZVP as well as Gibbs free energies G at 0, 300 and 600 K (data for isomer B are also listed in **Table S3**).

	PBE					TPSS				
	B			T		B			T	
	E	$G_0$	$G_{300}$	$G_{600}$	E	E	$G_0$	$G_{300}$	$G_{600}$	E
La	5.5	5.2	1.8	-2.1	10.88	9.7	9.4	7.1	4.4	14.56
Ce	4.7	4.4	0.9	-2.9	10.17	9.1	8.7	7.1	5.1	13.94
Pr	3.9	3.6	0.1	-3.9	9.45	8.5	8.1	7.4	6.3	13.29
Nd	3.2	2.9	-0.7	-4.7	8.89	8.1	7.8	6.3	4.5	12.93
Pm	2.8	2.5	-1.1	-5.2	8.56	7.8	7.4	4.2	0.5	12.75
Sm	2.2	1.9	-1.8	-5.8	8.14	7.4	7.0	3.6	-0.2	12.41
Eu	1.7	1.3	-2.4	-6.6	7.74	7.1	6.6	2.9	-1.5	12.09
Gd	1.3	0.9	-2.8	-7.0	7.43	6.9	6.4	1.8	-3.3	11.91
Tb	0.8	0.5	-3.3	-7.6	7.07	6.6	6.1	1.7	-3.2	11.58
Dy	0.5	0.2	-3.7	-8.0	6.78	6.4	5.9	1.4	-3.7	11.36
Ho	0.1	-0.3	-4.2	-8.5	6.44	6.1	5.6	1.0	-4.2	11.06
Er	-0.5	-0.9	-4.7	-9.0	6.03	5.7	5.2	0.5	-4.8	10.69
Tm	-0.8	-1.1	-5.0	-9.4	5.79	5.5	5.0	0.2	-5.2	10.47
Yb	-1.5	-1.9	-5.8	-10.1	5.29	4.8	4.3	-0.4	-5.7	9.94
Lu	-2.2	-2.6	-6.4	-10.7	4.96	4.2	3.7	-1.0	-6.3	9.56

The zero-point energy ( $G(T=0K)-E$ ) is almost negligible, amounting to 0.6 kJ/mol at most. In contrast,  $G(T=300K)$  differs from the bare electronic energies by a few kJ/mol. The favouring of A over B becomes smaller by typically 3...5 kJ/mol (which actually means a disfavouring of A for the heavier lanthanides), and the energy difference of the transition state T to A increases by about the same amount, which is also similar to the difference between PBE and TPSS. At 600K these effects are about three times larger. The results are graphically displayed in **Figure S3**; they suggest that by the calculation of the Gibbs free energy at 300 K with PBE/ECP/TZVP or TPSS/ECP/TZVP the energetic situation in the experiment is reproduced with an accuracy of approx. 10 kJ/mol, whereby the greatest uncertainty arises from the choice of the functional; thus, in the following data for both functionals are calculated and listed.

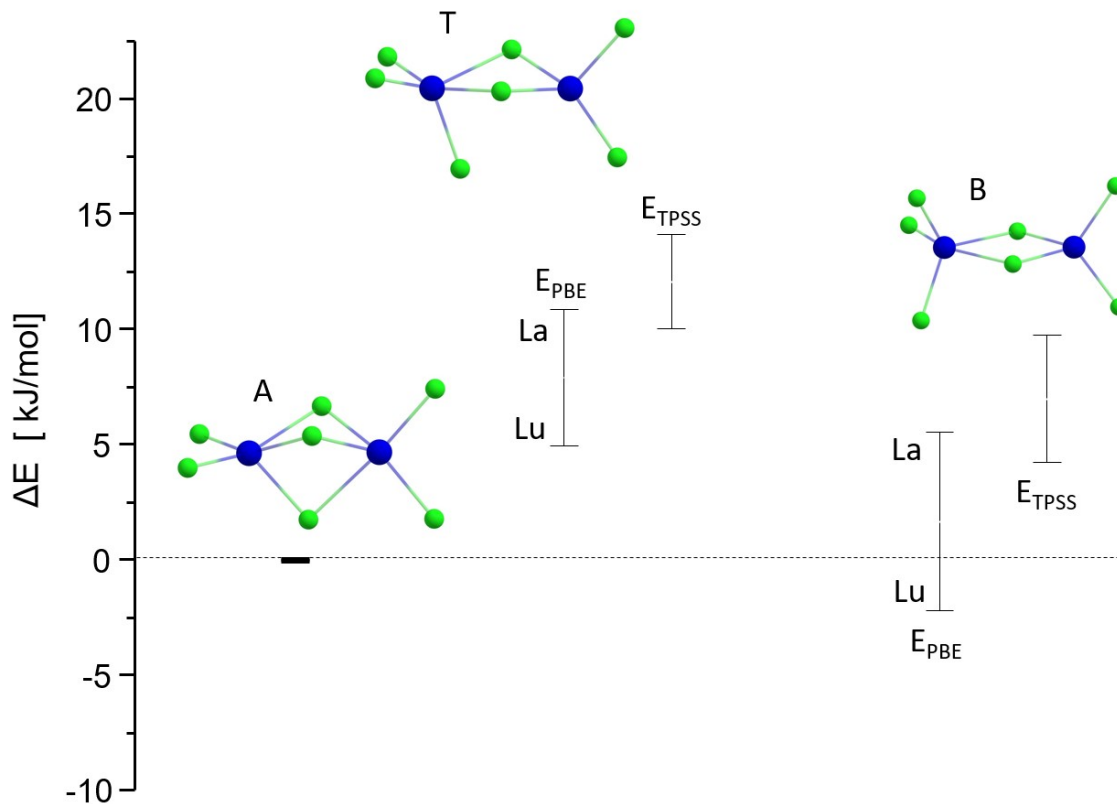


**Figure S4.** Energies E of isomer B and transition state T relative to isomer A for La-Lu at levels PBE/ECP/TZVP and TPSS/ECP/TZVP.

**Relative energies and Gibbs free energies of minima (relative to the minimum with lowest energy for Ln=La).** In the following we list the energies and Gibbs free energies of the most stable isomers of  $\text{Ln}_x\text{Cl}_{3x+1}^-$ ,  $\text{Ln}=\text{La-Lu}$ , separately for  $x=2-6$  and graphically display the PBE data for E and G(300K).

**Table S3.** Isomers of  $\text{Ln}_2\text{Cl}_7^-$ ,  $\text{Ln}=\text{La-Lu}$ . Energies E and Gibbs free energies, G, for T=0, 300, 600 K of isomers B and C relative to isomer A, in kJ/mol at levels PBE/ECP/TZVP and TPSS/ECP/TZVP (data for isomer B are also listed in **Table S2**).

	PBE							TPSS								
	B				C				B				C			
	E	G <sub>0</sub>	G <sub>300</sub>	G <sub>600</sub>	E	G <sub>0</sub>	G <sub>300</sub>	G <sub>600</sub>	E	G <sub>0</sub>	G <sub>300</sub>	G <sub>600</sub>	E	G <sub>0</sub>	G <sub>300</sub>	G <sub>600</sub>
La	5.5	5.2	1.8	-2.1	32.2	31.7	33.3	34.4	9.7	9.4	7.1	4.4	38.0	37.5	40.7	43.3
Ce	4.7	4.4	0.9	-2.9	31.4	31.0	32.7	33.8	9.1	8.7	7.1	5.1	37.2	36.7	40.7	44.1
Pr	3.9	3.6	0.1	-3.9	30.6	30.2	31.8	33.0	8.5	8.1	7.4	6.3	36.3	35.9	40.9	45.4
Nd	3.2	2.9	-0.7	-4.7	29.8	29.4	31.2	32.5	8.1	7.8	6.3	4.5	35.6	35.3	39.9	44.1
Pm	2.8	2.5	-1.1	-5.2	29.4	29.0	30.8	32.1	7.8	7.4	4.2	0.5	35.3	35.0	38.1	40.8
Sm	2.2	1.9	-1.8	-5.8	28.9	28.5	30.2	31.5	7.4	7.0	3.6	-0.2	34.8	34.5	37.7	40.6
Eu	1.7	1.3	-2.4	-6.6	28.5	28.0	29.7	31.0	7.1	6.6	2.9	-1.5	34.4	34.0	37.0	39.6
Gd	1.3	0.9	-2.8	-7.0	28.1	27.7	29.4	30.7	6.9	6.4	1.8	-3.3	34.1	33.6	36.0	37.8
Tb	0.8	0.5	-3.3	-7.6	27.7	27.3	29.2	30.5	6.6	6.1	1.7	-3.2	33.7	33.3	35.9	38.1
Dy	0.5	0.2	-3.7	-8.0	27.5	27.1	29.0	30.5	6.4	5.9	1.4	-3.7	33.4	33.0	35.7	37.9
Ho	0.1	-0.3	-4.2	-8.5	27.2	26.8	28.8	30.3	6.1	5.6	1.0	-4.2	33.0	32.6	35.5	37.9
Er	-0.5	-0.9	-4.7	-9.0	26.8	26.4	28.4	29.9	5.7	5.2	0.5	-4.8	32.6	32.3	35.4	38.0
Tm	-0.8	-1.1	-5.0	-9.4	26.6	26.2	28.1	29.6	5.5	5.0	0.2	-5.2	32.4	32.0	35.2	38.0
Yb	-1.5	-1.9	-5.8	-10.1	26.0	25.6	27.5	28.8	4.8	4.3	-0.4	-5.7	31.9	31.5	34.8	37.8
Lu	-2.2	-2.6	-6.4	-10.7	25.8	25.3	27.1	28.3	4.2	3.7	-1.0	-6.3	31.6	31.2	34.5	37.4

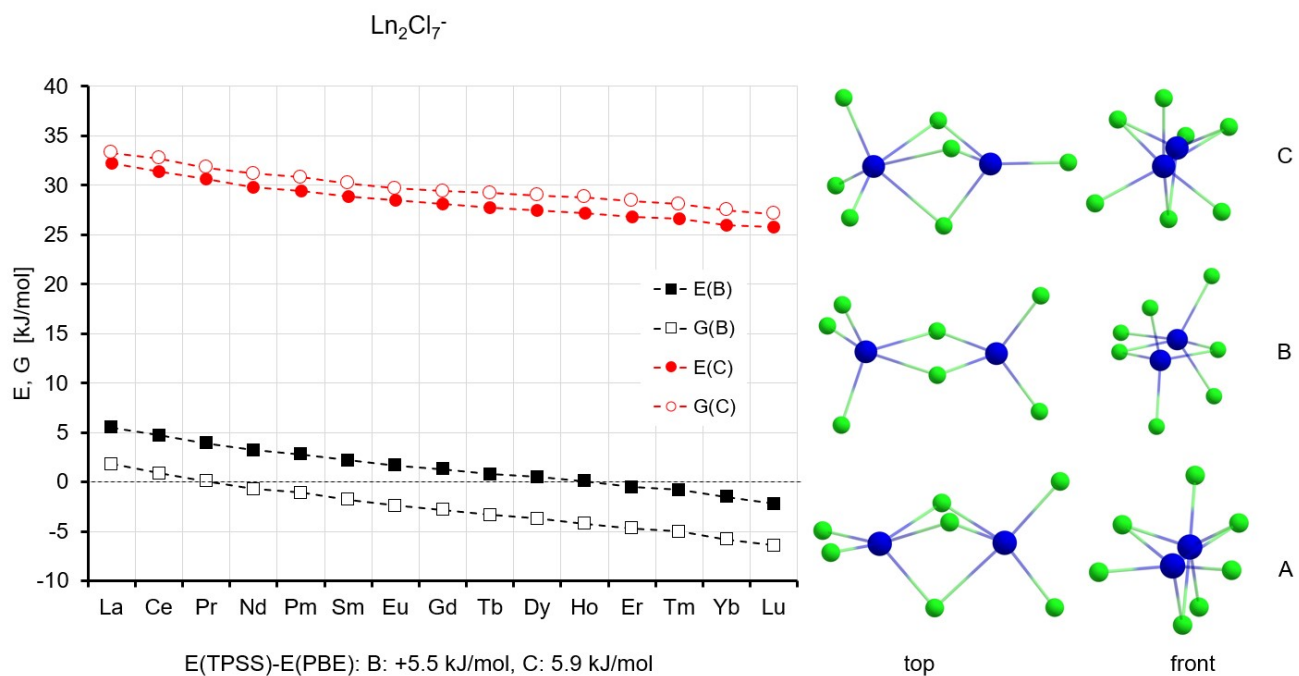


**Figure S5.**  $\text{Ln}_2\text{Cl}_7^-$ : Energies, E, and Gibbs free energies, G, at 300 K of isomer B and C relative to isomer A for La-Lu at levels PBE/ECP/TZVP and TPSS/ECP/TZVP.

**Table S4.** Relative energies and Gibbs free energies of isomers of  $\text{Ln}_3\text{Cl}_{10}^-$ , see also **Table S3**.

	PBE								TPSS							
	B				C				B				C			
	E	$G_0$	$G_{300}$	$G_{600}$												
La	17.8	17.2	10.9	3.9	24.8	24.7	15.9	7.1	22.1	21.6	15.8	9.5	20.5	20.6	15.9	11.3
Ce	17.6	17.1	10.5	3.2	25.1	25.0	16.0	7.1	22.3	21.6	15.2	8.2	20.7	20.8	14.9	9.2
Pr	17.5	16.9	10.4	3.2	25.8	25.7	17.5	9.2	22.5	21.7	14.8	7.1	21.6	21.5	14.8	8.0
Nd	17.4	16.8	10.2	2.8	26.3	26.2	18.0	9.8	22.8	22.0	13.1	3.3	22.0	21.9	14.4	6.8
Pm	17.2	16.6	10.0	2.7	26.2	26.1	17.4	8.6	22.8	22.0	15.2	7.5	21.9	21.8	12.7	3.6
Sm	17.0	16.4	10.2	3.4	26.3	26.1	16.4	6.5	22.8	22.0	15.4	8.0	21.9	21.8	12.8	3.8
Eu	16.8	16.2	9.5	2.2	26.6	26.1	14.0	1.6	22.9	22.1	14.4	5.8	22.3	22.1	13.0	3.7
Gd	16.7	16.1	9.5	2.2	25.8	25.1	10.8	-4.0	23.0	22.2	14.7	6.5	22.1	22.0	14.0	5.9
Tb	16.7	16.0	9.4	2.2	25.1	24.5	12.3	-0.4	23.2	22.3	14.8	6.5	21.9	21.5	12.2	2.7
Dy	16.8	16.1	9.6	2.4	24.5	23.9	12.6	0.9	23.6	22.7	15.8	8.0	21.7	21.1	11.5	1.5
Ho	16.6	15.9	9.2	1.9	23.9	23.2	12.6	1.3	23.6	22.7	15.6	7.5	21.2	20.6	10.6	0.0
Er	16.2	15.5	9.0	1.7	23.0	22.4	12.1	1.2	23.5	22.5	14.1	4.8	20.4	19.8	8.9	-2.5
Tm	16.2	15.5	8.7	1.1	22.3	21.7	11.8	1.3	23.7	22.7	14.2	4.7	20.0	19.3	7.9	-4.0
Yb	15.6	14.8	7.9	0.3	21.4	20.9	11.1	0.9	23.2	22.2	14.3	5.4	19.2	18.5	6.9	-5.3
Lu	14.9	14.2	7.3	-0.4	20.6	20.1	10.6	0.6	22.6	21.5	13.0	3.5	18.5	17.7	5.9	-6.6

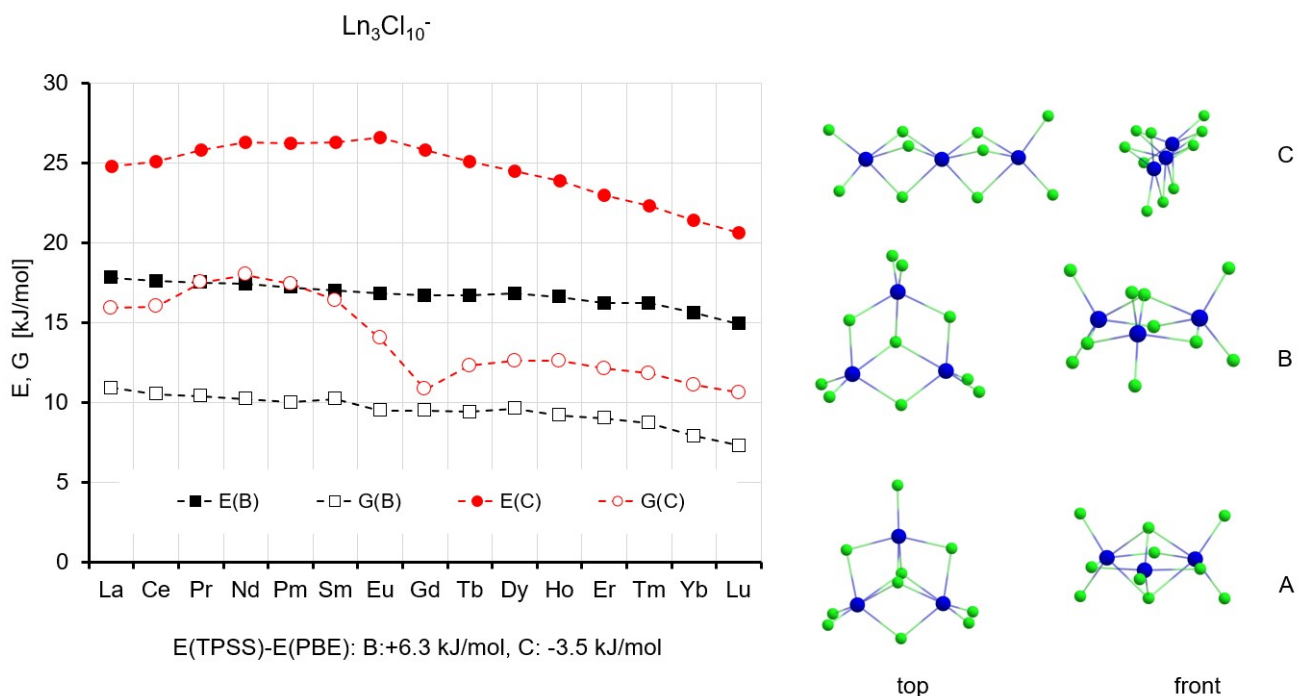


**Figure S6.**  $\text{Ln}_3\text{Cl}_{10}^-$ : Energies, E, and Gibbs free energies, G, at 300 K of isomer B and C relative to isomer A for La-Lu at levels PBE/ECP/TZVP and TPSS/ECP/TZVP.

**Table S5.** Relative energies and Gibbs free energies of isomers of  $\text{Ln}_4\text{Cl}_{13}^-$ , see also **Table S3**. Italic numbers indicate an imaginary frequency for the corresponding isomer.

	PBE								TPSS							
	B				C				B				C			
	E	$G_0$	$G_{300}$	$G_{600}$	E	$G_0$	$G_{300}$	$G_{600}$	E	$G_0$	$G_{300}$	$G_{600}$	E	$G_0$	$G_{300}$	$G_{600}$
La	15.5	14.7	5.7	-4.2	60.4	60.2	53.2	45.9	23.7	22.4	11.9	0.1	69.8	69.2	62.4	55.0
Ce	12.7	11.9	3.1	-6.6	58.9	58.7	51.7	44.5	20.8	19.6	9.5	-1.8	68.0	67.5	61.2	54.3
Pr	10.1	9.3	0.5	-9.1	57.2	57.1	49.9	42.4	18.0	16.9	7.2	-3.6	65.9	65.6	59.7	53.4
Nd	8.0	7.2	-1.5	-11.1	56.3	56.2	48.6	40.9	15.9	14.9	5.5	-4.9	64.7	64.5	58.7	52.7
Pm	6.1	5.3	-3.3	-12.8	55.9	55.7	48.0	40.1	13.9	12.9	3.7	-6.6	63.9	63.7	57.8	51.6
Sm	3.8	3.1	-5.3	-14.5	55.4	55.3	47.5	39.5	11.7	10.7	1.5	-8.8	63.3	63.0	56.9	50.5
Eu	1.9	1.2	-7.0	-15.9	54.9	54.8	47.0	39.0	9.6	8.6	-0.6	-10.9	62.5	62.2	56.0	49.5
Gd	-0.1	-0.8	-8.7	-17.4	54.5	54.4	46.3	38.0	7.5	6.5	-2.5	-12.6	61.9	61.6	55.5	49.0
Tb	-2.1	-2.7	-10.4	-18.9	54.0	54.0	45.0	35.8	5.4	4.5	-4.2	-13.9	61.2	61.0	55.0	48.9
Dy	-3.7	-4.2	-11.9	-20.2	<b>53.6</b>	<b>53.5</b>	<b>54.4</b>	<b>58.6</b>	3.7	2.8	-5.6	-14.9	60.5	60.3	54.5	48.4
Ho	-5.5	-6.1	-13.6	-21.8	<b>53.2</b>	<b>53.1</b>	<b>54.0</b>	<b>58.1</b>	1.6	0.9	-7.3	-16.3	59.8	59.7	53.6	47.3
Er	-7.6	-8.2	-15.5	-23.5	<b>52.9</b>	<b>52.8</b>	<b>53.6</b>	<b>57.7</b>	-0.6	-1.4	-9.3	-18.0	59.4	59.3	52.5	45.5
Tm	-9.1	-9.6	-16.8	-24.8	<b>52.7</b>	<b>52.6</b>	<b>53.3</b>	<b>57.3</b>	-2.1	-2.8	-10.7	-19.3	59.0	58.8	51.0	42.9
Yb	-11.3	-11.8	-18.9	-26.6	<b>52.4</b>	<b>52.3</b>	<b>53.0</b>	<b>56.9</b>	-4.6	-5.3	-13.0	-21.5	<b>58.6</b>	<b>58.3</b>	<b>59.2</b>	<b>63.2</b>
Lu	-12.4	-12.9	-19.8	-27.4	<b>52.5</b>	<b>52.4</b>	<b>53.0</b>	<b>56.8</b>	-5.8	-6.6	-14.2	-22.6	<b>58.6</b>	<b>58.2</b>	<b>58.9</b>	<b>62.7</b>

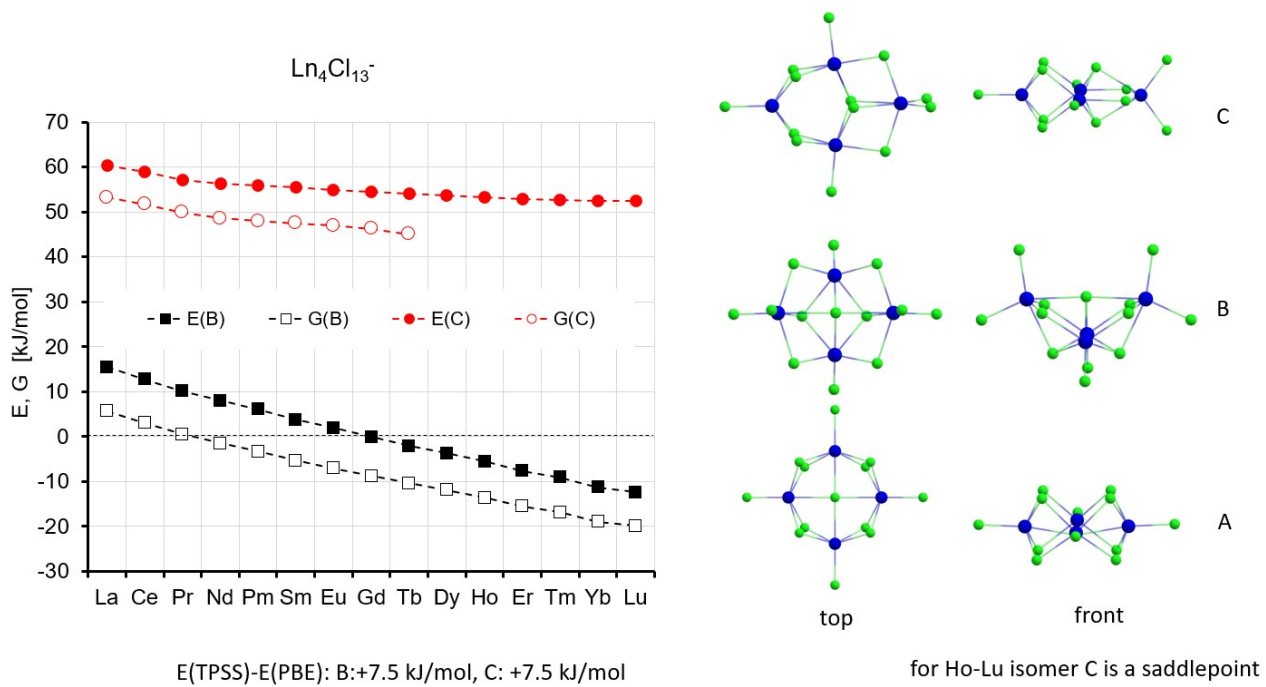


**Figure S7.**  $\text{Ln}_4\text{Cl}_{13}^-$ : Energies, E, and Gibbs free energies, G, at 300 K of isomer B and C relative to isomer A for La-Lu at levels PBE/ECP/TZVP and TPSS/ECP/TZVP.

**Table S6.** Relative energies and Gibbs free energies of isomers of  $\text{Ln}_5\text{Cl}_{16}^-$ , see also **Table S3**.

	PBE								TPSS							
	B				C				B				C			
	E	$G_0$	$G_{300}$	$G_{600}$	E	$G_0$	$G_{300}$	$G_{600}$	E	$G_0$	$G_{300}$	$G_{600}$	E	$G_0$	$G_{300}$	$G_{600}$
La	-1.3	-0.6	10.6	22.5	-1.2	0.3	11.7	24.6	-4.6	-4.0	5.2	15.1	-10.5	-8.9	1.7	13.8
Ce	2.4	3.2	14.5	26.7	4.0	5.5	16.9	29.8	-1.6	-0.9	9.2	20.1	-6.0	-4.3	6.8	19.5
Pr	6.1	6.9	18.5	31.0	9.3	10.7	22.2	35.0	1.2	2.1	12.9	24.7	-1.5	0.3	11.9	25.1
Nd	10.0	10.8	22.7	35.4	14.7	16.2	27.5	40.3	4.6	5.5	16.3	28.1	3.5	5.2	16.7	29.9
Pm	13.9	14.8	26.7	39.6	20.2	21.6	32.8	45.3	8.1	9.0	19.7	31.4	8.7	10.4	21.5	34.3
Sm	17.8	18.7	30.9	44.1	25.7	27.1	38.2	50.7	11.7	12.6	23.5	35.3	14.1	15.7	26.6	39.1
Eu	21.8	22.8	35.3	48.9	31.4	32.8	44.0	56.6	15.3	16.3	27.5	39.7	19.4	21.1	32.0	44.4
Gd	25.6	26.6	39.7	53.8	36.7	38.1	49.7	62.6	18.9	19.9	31.5	44.2	24.6	26.3	37.4	50.1
Tb	29.9	30.9	44.8	59.7	42.5	43.9	56.1	69.8	22.9	24.0	36.0	49.2	30.3	32.0	43.4	56.4
Dy	33.8	34.9	51.2	68.8	48.1	49.5	64.0	79.9	26.5	27.7	40.5	54.4	35.7	37.5	49.4	62.9
Ho	38.1	39.3	59.7	81.3	53.8	55.4	73.6	93.3	30.5	31.9	52.3	74.1	41.4	43.3	62.7	84.0
Er	42.2	43.5	64.5	86.9	59.6	61.1	79.7	99.7	34.7	36.0	55.4	76.1	47.3	49.2	67.3	87.2
Tm	46.2	47.4	65.3	84.5	65.1	66.4	81.5	98.0	38.8	40.2	52.3	62.4	53.0	54.9	65.5	74.5
Yb	50.3	51.4	68.1	86.1	70.7	71.9	85.3	99.9	42.9	44.3	57.1	67.9	58.8	60.7	71.6	80.8
Lu	53.3	54.5	70.5	87.8	75.1	76.3	88.5	101.8	46.3	47.6	68.4	90.5	63.9	65.5	84.0	104.2

Relative intensities for the  $\text{La}_5\text{Cl}_{16}^-$  isomers:

With the PBE functional the free energy of isomer B at 300 K is 10.6 kJ/mol above isomer A, isomer C is 11.7 kJ/mol higher. This translates into relative intensities of 98% for isomer A, 1% for B and 1% for C, respectively. With the TPSS functional the free energies are 5.2 kJ/mol and 1.7 kJ/mol, respectively (see also table S6). This in turn translates into relative intensities of 61% for isomer A, 8% for B and 31% for C. Both functionals differ by 5-10 kJ/mol and we cannot safely predict which isomer is preferred. For the later lanthanides, isomer A is strongly favoured.

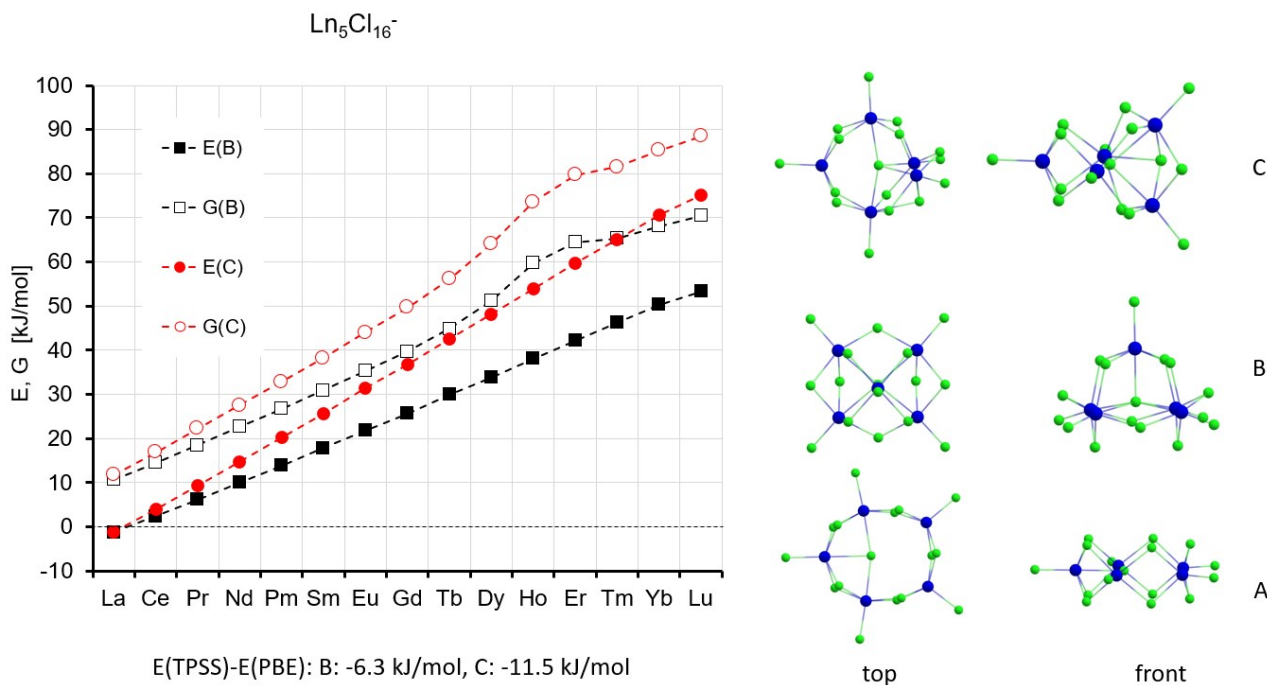


**Figure S8.**  $\text{Ln}_5\text{Cl}_{16}^-$ : Energies, E, and Gibbs free energies, G, at 300 K of isomer B and C relative to isomer A for La-Lu at levels PBE/ECP/TZVP and TPSS/ECP/TZVP.

**Table S7.** Relative energies and Gibbs free energies of isomers of  $\text{Ln}_6\text{Cl}_{19}^-$ , see also **Table S3**.

	PBE								TPSS							
	B				C				B				C			
	E	$G_0$	$G_{300}$	$G_{600}$												
La	21.3	21.2	6.9	-7.5	33.7	34.8	22.6	11.4	19.8	19.9	10.2	0.6	13.7	14.8	2.0	-9.9
Ce	20.3	20.0	1.4	-17.6	35.7	36.7	25.0	14.3	19.3	19.0	6.3	-6.7	16.3	17.2	4.2	-8.0
Pr	19.5	19.4	5.5	-8.6	38.7	39.5	28.1	17.5	18.9	18.7	6.3	-6.4	19.9	20.7	7.4	-5.3
Nd	18.5	18.3	5.2	-8.2	40.2	41.0	29.5	18.8	18.1	17.9	6.0	-6.1	21.9	22.7	10.4	-1.2
Pm	17.5	17.4	4.8	-8.1	41.0	41.8	30.2	19.4	17.3	17.2	5.8	-5.8	23.2	24.0	12.7	2.0
Sm	16.5	16.3	4.0	-8.6	41.8	42.5	31.0	20.1	16.3	16.3	5.1	-6.2	24.5	25.4	14.1	3.6
Eu	15.6	15.4	3.2	-9.2	43.2	43.9	32.2	21.1	15.6	15.5	4.2	-7.4	26.5	27.4	15.9	5.2
Gd	14.5	14.3	2.3	-9.9	43.7	44.3	32.5	21.2	14.7	14.5	2.7	-9.3	27.7	28.4	16.8	5.8
Tb	13.5	13.3	1.5	-10.6	44.6	45.1	33.0	21.4	13.9	13.5	1.4	-11.1	29.2	29.8	17.8	6.3
Dy	12.9	12.6	1.0	-11.0	45.9	46.3	33.9	21.9	13.6	13.1	0.6	-12.3	31.5	31.8	19.2	6.9
Ho	12.0	11.8	0.3	-11.4	46.9	47.2	34.6	22.3	12.9	12.3	-0.2	-13.3	33.2	33.2	18.6	4.0
Er	11.0	10.8	-0.4	-12.0	47.5	47.8	35.0	22.5	12.1	11.5	-0.9	-13.9	34.6	34.4	19.6	4.6
Tm	10.3	10.1	-1.0	-12.4	48.6	48.8	35.9	23.1	11.6	11.0	-1.2	-14.1	36.5	36.3	22.4	8.2
Yb	9.3	9.1	-1.9	-13.3	49.3	49.4	36.4	23.5	10.7	10.2	-1.8	-14.5	37.9	37.8	23.8	9.8
Lu	8.5	8.2	-2.7	-14.0	49.5	49.5	36.5	23.6	9.9	9.4	-2.6	-15.0	38.4	38.2	24.5	10.7

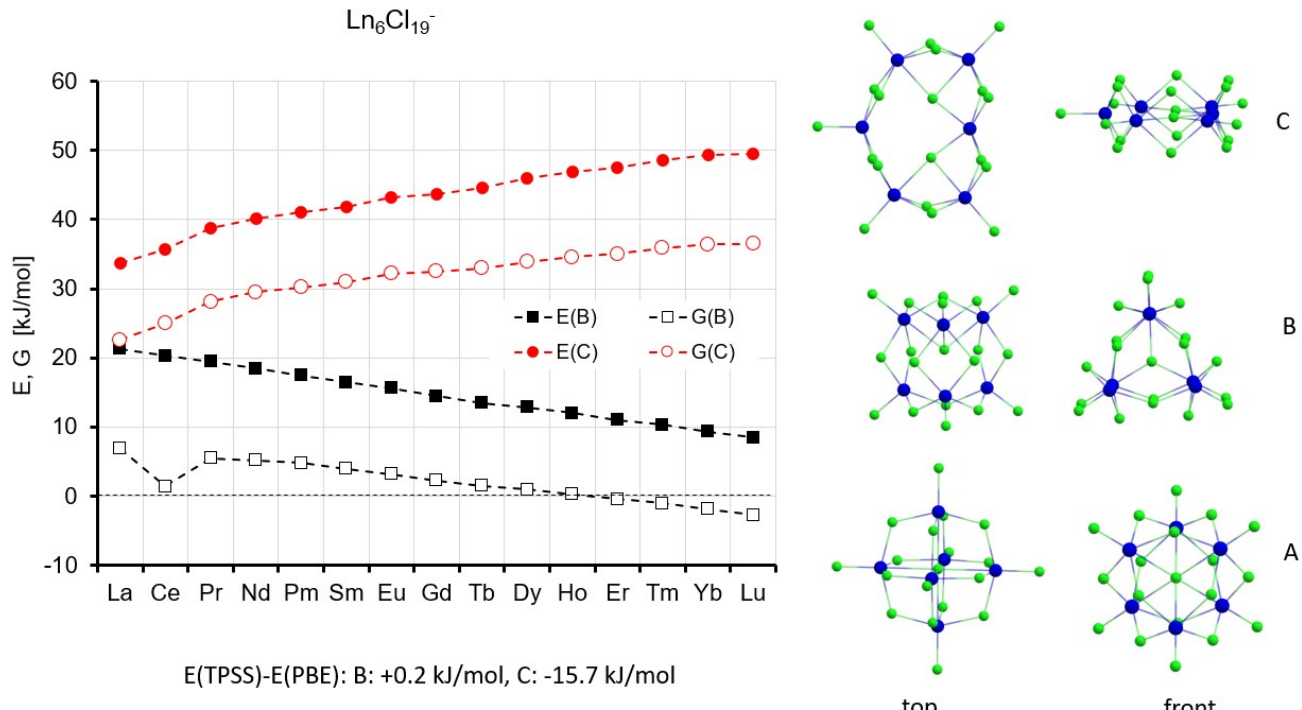


**Figure S9.**  $\text{Ln}_6\text{Cl}_{19}^-$ : Energies, E, and Gibbs free energies, G, at 300 K of isomer B and C relative to isomer A for La-Lu at levels PBE/ECP/TZVP and TPSS/ECP/TZVP.

**Reaction pathways and transition states.** In the Figures S10-S13 we graphically show the result of the reaction path optimizations at level PBE/lcecp-1-TZVP for  $\text{Ln}=\text{La}$  in case of  $x=3,4,5$  and  $\text{Ln}=\text{Lu}$  for  $x=6$ . All maxima show a single imaginary frequency already after this first step. Data for the transition states after final optimization (same convergence criteria as for the minima) are listed in **Tables S8** and **S9**. We note that the energies of the finally optimized transition states differ by that of the maxima in the path optimization typically by only  $\sim 1$  kJ/mol. For  $x=5$ , the pathways  $\text{A}\rightarrow\text{C}$  and  $\text{C}\rightarrow\text{B}$  were optimized separately and combined for the figure afterwards; we were not able to identify a direct path from  $\text{A}$  to  $\text{B}$  with low barrier.

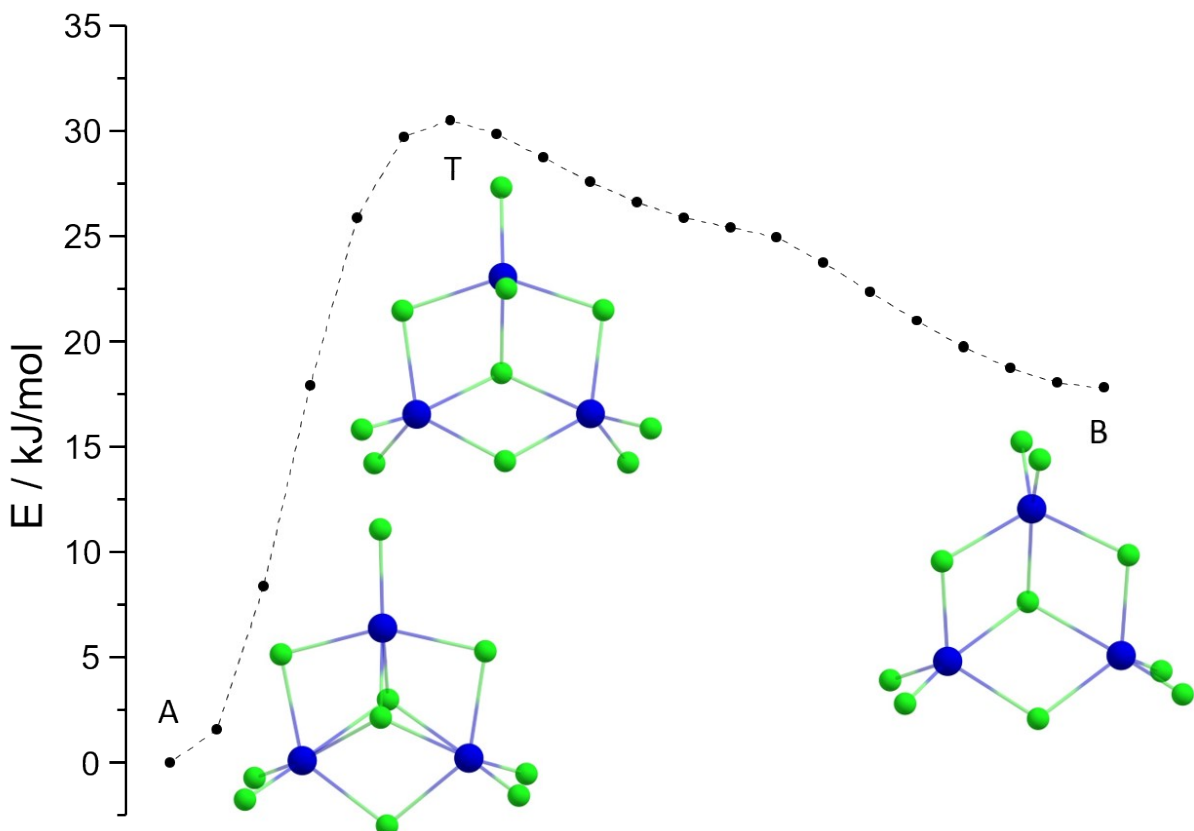


**Figure S10.** Optimized pathway from isomer A to isomer B for  $\text{La}_3\text{Cl}_{10}^-$  obtained at level PBE/lcecp-1-TZVP. Data for the finally optimized transition state for  $\text{Ln}=\text{La-Lu}$  are listed in **Table S8**.

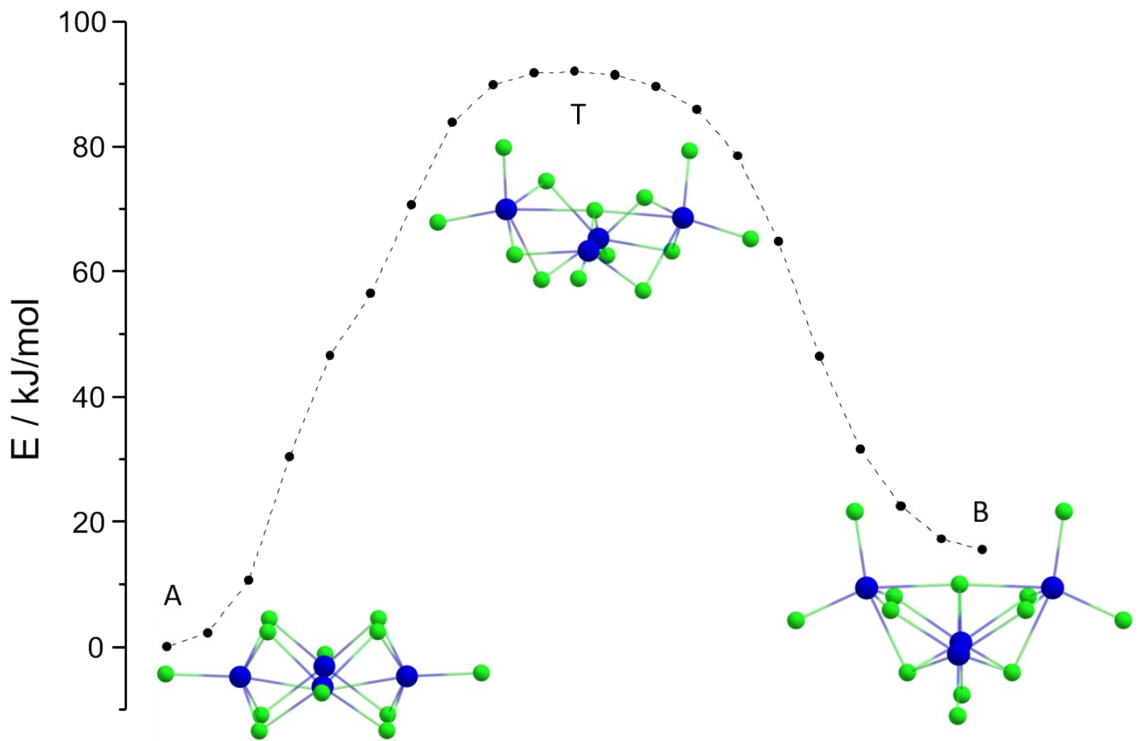


**Figure S11.** Optimized pathway from isomer A to isomer B for  $\text{La}_4\text{Cl}_{13}^-$  obtained at level PBE/1cecp-1-TZVP. Data for the finally optimized transition state for  $\text{Ln}=\text{La-Lu}$  are listed in **Table S8**.

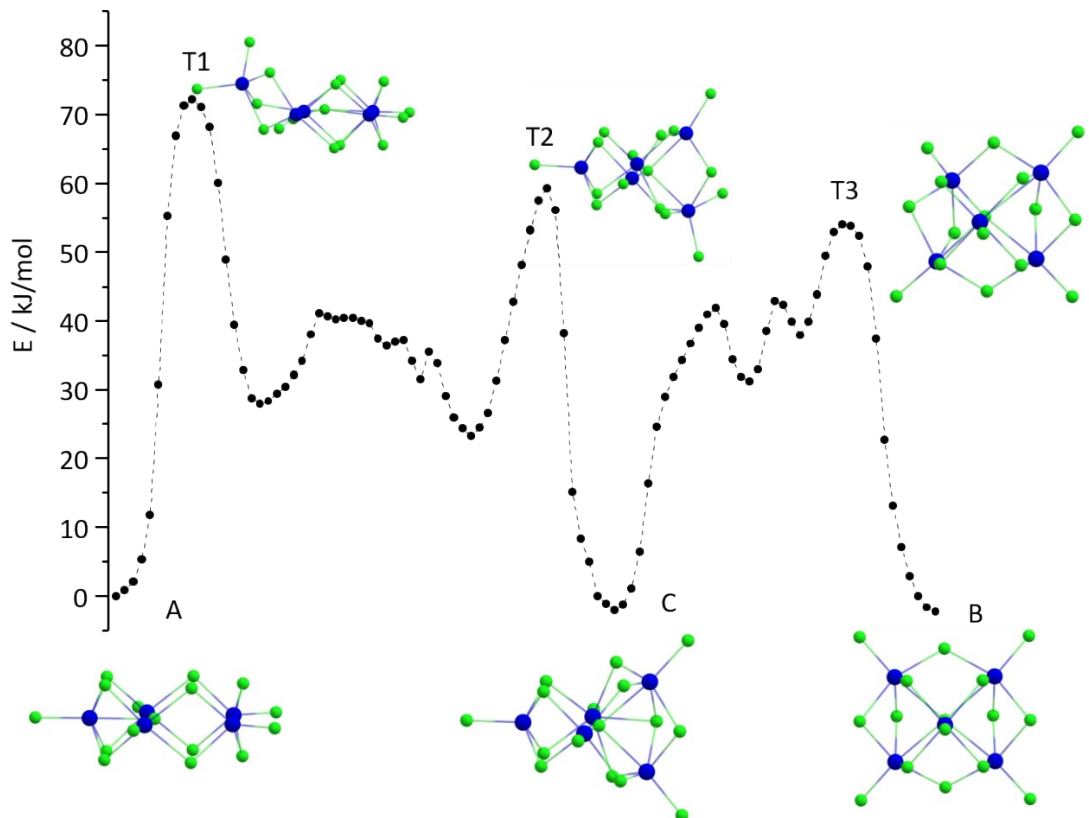


**Figure S12.** Optimized pathway from isomer A to isomer B via isomer C for  $\text{La}_5\text{Cl}_{16}^-$  obtained at level PBE/1cecp-1-TZVP. Data for the finally optimized transition states T1 and T2 for  $\text{Ln}=\text{La-Lu}$  are listed in **Table S9**.

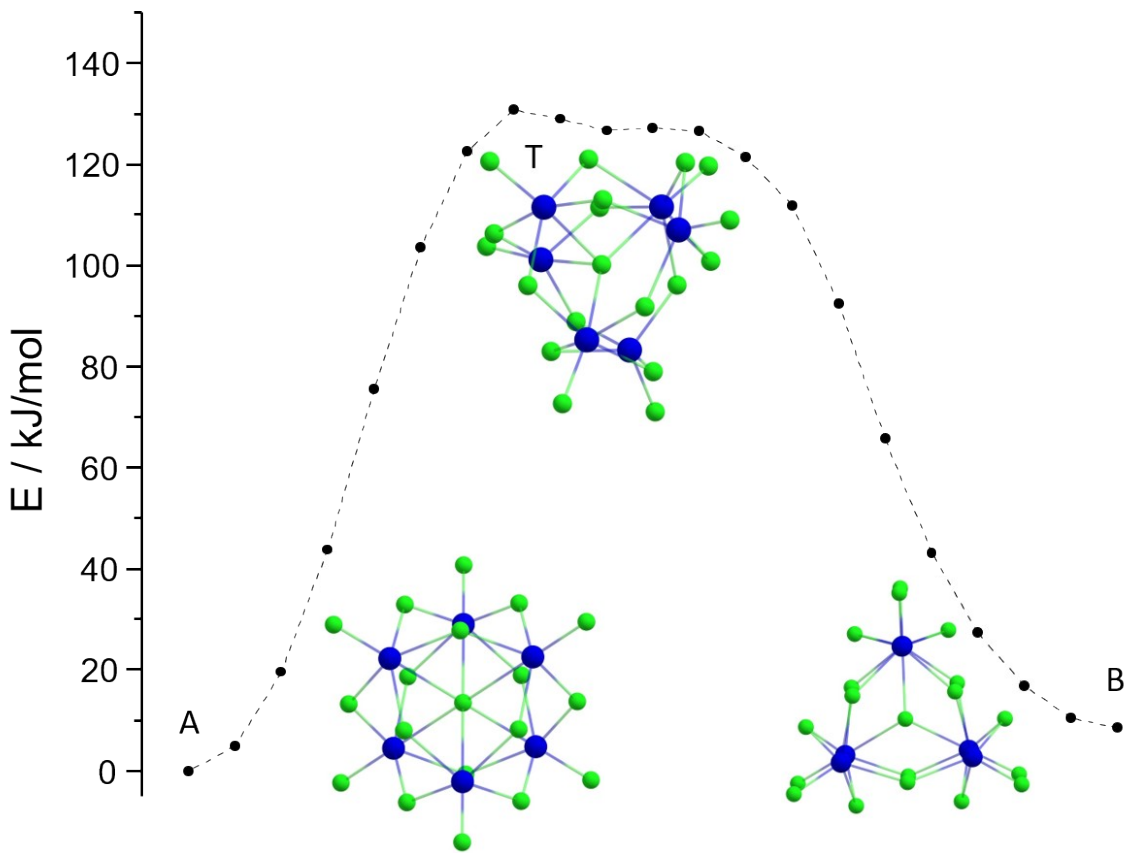


**Figure S13.** Optimized pathway from isomer A to isomer B for  $\text{Lu}_6\text{Cl}_{19}^-$  obtained at level PBE/1cecp-1-TZVP. Data for the finally optimized transition state for  $\text{Ln}=\text{La-Lu}$  are listed in **Table S8**.

**Table S8.** Energies (in  $\text{kJ/mol}$ ) of the transition state from A to B relative to isomer A at level PBE for  $x=2-4, 6$ , i.e.  $\text{Ln}_2\text{Cl}_7^-$ ,  $\text{Ln}_3\text{Cl}_{10}^-$ ,  $\text{Ln}_4\text{Cl}_{13}^-$  and  $\text{Ln}_6\text{Cl}_{19}^-$ .

	2	3	4	6
	E	E	E	E
La	10.9	25.2	90.5	82.9
Ce	10.2	25.2	87.3	86.3
Pr	9.4	25.1	84.2	90.0
Nd	8.9	25.1	81.6	93.3
Pm	8.6	25.2	79.4	96.6
Sm	8.1	25.2	76.8	99.8
Eu	7.7	25.2	74.4	103.2
Gd	7.4	25.4	72.0	106.1
Tb	7.1	25.5	69.6	109.4
Dy	6.8	25.8	67.5	112.9
Ho	6.4	25.8	65.0	116.1
Er	6.0	25.8	62.4	119.3
Tm	5.8	26.0	60.4	122.5
Yb	5.3	25.6	57.7	125.4
Lu	5.0	25.1	56.2	127.5

**Table S9.** Energies (in kJ/mol) of the transition states T1-T3 isomer A at level PBE for  $\text{Ln}_5\text{Cl}_{16}^-$ , Ln=La-Gd. For the heavier lanthanides T1 converges to A during the optimization.

	T1	T2	T3
	E	E	E
La	71.9	58.9	54.8
Ce	72.6	62.0	57.5
Pr	72.3	65.3	60.3
Nd	73.5	68.9	63.4
Pm	74.6	72.8	66.6
Sm	75.5	76.6	69.6
Eu	76.8	80.5	72.9
Gd	77.9	84.2	75.9

**Table S10.** Lowest (lo) and highest (hi) vibrational frequencies (in 1/cm) for low energy isomers of  $\text{Ln}_n\text{Cl}_{3n+1}^-$  ( $n = 2-6$ , Ln = La, Gd ,Lu) A, B and C (for n=5) as well as imaginary (im), lowest and highest vibrational frequency for the connecting transition states (Tr(A-B) etc.).

	A		B		Tr(A-B)												
	lo	hi	lo	hi	im	lo	hi										
n=2																	
La	12	291	10	298	-32	12	297										
Gd	13	300	10	308	-35	13	306										
Lu	15	308	11	316	-36	12	313										
n=3																	
La	21	302	15	305	-26	16	305										
Gd	24	312	17	316	-25	18	315										
Lu	27	319	18	323	-25	20	322										
n=4																	
La	20	307	22	309	-13	15	308										
Gd	24	318	25	320	-11	17	318										
Lu	28	326	27	327	-15	4	326										
n=6																	
La	36	318	14	317	-37	16	317										
Gd	40	329	22	327	-39	20	327										
Lu	44	335	27	334	-42	21	333										
n=5																	
	A		B		C		Tr1(A-C)			Tr2(A-C)			Tr(B-C)				
La	9	312	20	313	24	313	-20	6	313	-29	14	313	-19	19	314		
Gd	12	323	23	324	27	323	-14	9	323	-36	17	324	-18	25	324		
Lu	11	330	26	331	28	331	-1	2	326	-41	21	332	-25	30	332		

### Coordinates (PBE/ECP/TZVP, in Å)

$\text{LaCl}_4^-$

La	0.00000	-0.00000	0.00000
Cl	1.54718	-1.54718	1.54718
Cl	-1.54718	1.54718	1.54718
Cl	-1.54718	-1.54718	-1.54718
Cl	1.54718	1.54718	-1.54718

$\text{La}_2\text{Cl}_7^-$

isomer A

La	0.0393325	1.9941234	0.0342456
La	-0.0546563	-1.9942526	-0.0202587
Cl	2.1010511	0.1809318	0.2129749
Cl	-1.2827735	0.0062668	1.6232989
Cl	-0.6980199	-0.1875816	-1.9943008
Cl	1.9982567	-3.6840657	-0.0042657
Cl	-2.0985110	-3.6806370	0.0622151
Cl	0.4272561	3.6897503	2.0350149
Cl	-0.4319357	3.6754646	-1.9710416

isomer B

La	-0.0159202	2.4237904	-0.0554668
La	0.0116743	-2.0302300	0.0401069
Cl	2.4401933	3.2505990	0.4906635
Cl	0.4984255	-0.0275493	1.7927335
Cl	-0.4840048	-0.0176003	-1.7491287
Cl	2.1097366	-3.5161930	-0.5561431
Cl	-2.0972979	-3.5129446	0.6050371
Cl	-1.8200497	3.2514386	1.6981129
Cl	-0.6427571	3.7689505	-2.2565372

isomer C

La	0.0000000	0.0000000	2.2179740
La	0.0000000	0.0000000	-1.7921214
Cl	0.0000000	0.0000000	4.8924532
Cl	1.0856153	1.8803409	0.6638417
Cl	1.0856153	-1.8803409	0.6638417
Cl	-2.1712307	0.0000000	0.6638417
Cl	-1.2146923	-2.1039088	-2.8508434
Cl	-1.2146923	2.1039088	-2.8508434
Cl	2.4293847	0.0000000	-2.8508434

transition state A-B

La	0.1650438	2.0056446	-0.0223381
La	-0.2992653	-2.2072320	0.0201946
Cl	2.5832290	0.9155576	0.0628229
Cl	-0.7650935	-0.2087044	1.8297752
Cl	-0.6878661	-0.2485048	-1.8532650
Cl	1.8871282	-3.6879243	0.0779475
Cl	-2.3771993	-3.8284277	-0.0016077
Cl	-0.3249392	3.6548711	2.0050331
Cl	-0.1810376	3.6047198	-2.1185626

$\text{La}_3\text{Cl}_{10}^-$

isomer A

La	0.0000000	-2.2165520	1.0862448
La	-0.0000000	-0.0000000	-2.4260977
La	0.0000000	2.2165520	1.0862448
Cl	0.0000000	-2.7235926	-1.7790184

Cl -2.0915155 -3.6270305 1.8359722  
 Cl -0.0000000 -0.0000000 2.8698144  
 Cl 2.0915155 -3.6270305 1.8359722  
 Cl -0.0000000 -0.0000000 -5.0718876  
 Cl -2.0915155 3.6270305 1.8359722  
 Cl 2.0915155 3.6270305 1.8359722  
 Cl 1.8141398 -0.0000000 -0.2950529  
 Cl 0.0000000 2.7235926 -1.7790184  
 Cl -1.8141398 -0.0000000 -0.2950529  
 isomer B  
 La 1.3329406 2.3087209 -0.0180813  
 La 1.3329406 -2.3087209 -0.0180813  
 La -2.6658813 0.0000000 -0.0180813  
 Cl 2.1299029 -3.6891000 2.0727217  
 Cl 0.0000000 0.0000000 -1.3875387  
 Cl 2.8789027 0.0000000 0.6084345  
 Cl 2.1299029 3.6891000 2.0727217  
 Cl 2.0976632 3.6332592 -2.1477982  
 Cl -1.4394514 2.4932029 0.6084345  
 Cl -4.2598058 0.0000000 2.0727217  
 Cl -1.4394514 -2.4932029 0.6084345  
 Cl -4.1953264 0.0000000 -2.1477982  
 Cl 2.0976632 -3.6332592 -2.1477982  
 isomer C  
 La 3.9530168 -0.0539669 -0.0025827  
 La -0.0000034 0.1241195 0.0000499  
 La -3.9530136 -0.0539703 0.0025474  
 Cl 5.7417853 0.8072444 -1.7508963  
 Cl 2.0345894 1.1496354 1.7276194  
 Cl -1.9155352 -2.0178659 0.1846965  
 Cl 5.4745764 -1.1277093 1.8711988  
 Cl 1.9155511 -2.0178430 -0.1847960  
 Cl -5.7418890 0.8072025 1.7507812  
 Cl -5.4744431 -1.1277107 -1.8713344  
 Cl -2.0345921 1.1497925 -1.7274830  
 Cl -1.8524279 1.1568452 1.7882803  
 Cl 1.8523861 1.1570041 -1.7881236  
 transition state A-B  
 La -2.1868550 1.1770192 -0.5381080  
 La -0.1611262 -2.5569683 0.5737798  
 La 2.1883506 1.4238003 -0.2728560  
 Cl -2.7708146 -1.5710087 0.0112953  
 Cl -4.2816518 2.1401190 -1.8235907  
 Cl -0.0522223 3.0343538 -0.9694992  
 Cl -1.9513488 1.5865856 2.0428399  
 Cl 0.4682560 -4.5485487 -1.0086058  
 Cl 3.9095993 1.2760575 -2.2431347  
 Cl 3.2798725 2.9909347 1.5312083  
 Cl -0.6162952 -3.6181065 2.9337721  
 Cl 2.0998834 -0.9676202 1.2803548  
 Cl 0.0743521 -0.3666176 -1.5174558

$\text{La}_4\text{Cl}_{13}^-$   
 isomer A  
 La -2.0808417 -2.0808417 -0.0262336  
 La -2.0808417 2.0808417 -0.0262336  
 La 2.0808417 2.0808417 -0.0262336  
 La 2.0808417 -2.0808417 -0.0262336

Cl -3.2361407 0.0000000 -1.6526881  
 Cl 0.0000000 3.2361407 -1.6526881  
 Cl -2.7133056 0.0000000 1.8190772  
 Cl 0.0000000 -3.2361407 -1.6526881  
 Cl 0.0000000 -2.7133056 1.8190772  
 Cl 0.0000000 2.7133056 1.8190772  
 Cl -3.9381809 -3.9381809 0.0977385  
 Cl -0.0000000 0.0000000 -0.6453617  
 Cl 2.7133056 0.0000000 1.8190772  
 Cl 3.9381809 -3.9381809 0.0977385  
 Cl -3.9381809 3.9381809 0.0977385  
 Cl 3.2361407 0.0000000 -1.6526881  
 Cl 3.9381809 3.9381809 0.0977385  
 isomer B  
 La 0.0000000 -2.1558852 -1.0415380  
 La 0.0000000 2.1558852 -1.0415380  
 La 3.1482405 0.0000000 0.9967481  
 La -3.1482405 0.0000000 0.9967481  
 Cl -0.0000000 0.0000000 1.1619702  
 Cl 0.0000000 -3.9451541 -2.9538963  
 Cl 2.2789901 -2.7099893 0.4831470  
 Cl -2.2789901 -2.7099893 0.4831470  
 Cl 1.7654254 0.0000000 -1.8943174  
 Cl 2.2789901 2.7099893 0.4831470  
 Cl 3.5606112 0.0000000 3.5831557  
 Cl 5.5260811 0.0000000 -0.1067280  
 Cl -1.7654254 0.0000000 -1.8943174  
 Cl 0.0000000 3.9451541 -2.9538963  
 Cl -2.2789901 2.7099893 0.4831470  
 Cl -3.5606112 0.0000000 3.5831557  
 Cl -5.5260811 0.0000000 -0.1067280  
 isomer C  
 La -0.0000000 2.2824108 -0.1084416  
 La 0.0000000 -0.0000000 -3.5969426  
 La -0.0000000 -2.2824108 -0.1084416  
 La 0.0000000 -0.0000000 3.5680398  
 Cl 0.0000000 -0.0000000 -6.2196653  
 Cl -1.7419308 1.8133691 -2.3466642  
 Cl -0.0000000 4.8902970 -0.3686627  
 Cl 1.7419308 -1.8133691 -2.3466642  
 Cl 1.7419308 1.8133691 -2.3466642  
 Cl -0.0000000 2.7041399 2.6735263  
 Cl 1.6778530 -0.0000000 0.8490927  
 Cl -1.7419308 -1.8133691 -2.3466642  
 Cl -0.0000000 -2.7041399 2.6735263  
 Cl -1.6778530 -0.0000000 0.8490927  
 Cl 2.1199321 -0.0000000 5.1307173  
 Cl -2.1199321 -0.0000000 5.1307173  
 Cl -0.0000000 -4.8902970 -0.3686627  
 transition state A-B  
 La -2.3924360 1.4477244 -0.5907738  
 La 1.9969498 2.5090548 0.5164490  
 La 2.3895811 -1.4446479 -0.6099109  
 La -1.9944417 -2.5116421 0.5132037  
 Cl 0.9753541 3.2240963 2.8325607  
 Cl 3.4775846 0.1565718 1.3779855  
 Cl -0.3741681 3.3560414 -0.8870903  
 Cl -3.4710128 -0.1637363 1.3939853

Cl -2.3068786 -0.8358153 -2.0485697  
 Cl 2.2967926 0.8463875 -2.0554014  
 Cl -4.4313922 2.8871972 -1.3831543  
 Cl 0.0015027 -0.0016519 0.6341914  
 Cl 0.3698559 -3.3514378 -0.9061355  
 Cl -3.8236710 -4.2926737 -0.0959500  
 Cl 3.8233138 4.2930573 -0.0925411  
 Cl -0.9615756 -3.2384488 2.8206524  
 Cl 4.4246415 -2.8800770 -1.4195012

$\text{La}_5\text{Cl}_{16}^-$   
 isomer A  
 La -0.0000000 0.0000000 3.7785299  
 La 0.0000000 -3.0698976 1.1054878  
 La 0.0000000 -2.1535486 -3.0650452  
 La 0.0000000 2.1535486 -3.0650452  
 La 0.0000000 3.0698976 1.1054878  
 Cl -0.0000000 0.0000000 0.5818248  
 Cl -0.0000000 0.0000000 6.4003010  
 Cl -1.8183734 2.0502523 3.0230045  
 Cl 1.8096329 -3.0340573 -1.1271081  
 Cl 1.8183734 -2.0502523 3.0230045  
 Cl 0.0000000 -5.6293341 1.6548052  
 Cl -1.8183734 -2.0502523 3.0230045  
 Cl -1.8096329 -3.0340573 -1.1271081  
 Cl -1.7773103 0.0000000 -3.5298466  
 Cl 1.7773103 0.0000000 -3.5298466  
 Cl 0.0000000 -3.7453250 -5.1323985  
 Cl 0.0000000 3.7453250 -5.1323985  
 Cl -1.8096329 3.0340573 -1.1271081  
 Cl 0.0000000 5.6293341 1.6548052  
 Cl 1.8183734 2.0502523 3.0230045  
 Cl 1.8096329 3.0340573 -1.1271081  
 isomer B  
 La -2.4138740 2.0475805 0.7102564  
 La -2.4138740 -2.0475805 0.7102564  
 La 2.4138740 -2.0475805 0.7102564  
 La 0.0000000 0.0000000 -2.7938970  
 La 2.4138740 2.0475805 0.7102564  
 Cl -4.1442359 0.0000000 -0.2112343  
 Cl -4.0886602 -3.9472682 1.3501686  
 Cl -4.0886602 3.9472682 1.3501686  
 Cl -2.3255931 0.0000000 2.7123217  
 Cl 0.0000000 -3.3708154 1.4555061  
 Cl 4.0886602 -3.9472682 1.3501686  
 Cl 2.3255931 0.0000000 2.7123217  
 Cl 0.0000000 0.0000000 0.1942516  
 Cl 1.8454079 -2.0820703 -2.0694925  
 Cl -1.8454079 -2.0820703 -2.0694925  
 Cl 0.0000000 0.0000000 -5.4147994  
 Cl 1.8454079 2.0820703 -2.0694925  
 Cl 4.1442359 0.0000000 -0.2112343  
 Cl 0.0000000 3.3708154 1.4555061  
 Cl 4.0886602 3.9472682 1.3501686  
 Cl -1.8454079 2.0820703 -2.0694925  
 isomer C  
 La 2.2658670 -0.2982282 2.1054322  
 La 2.2658670 -0.2982282 -2.1054322

La 0.0629929 2.8870142 -0.0000000  
 La -3.5097589 0.5698569 -0.0000000  
 La -1.1012181 -2.9376944 -0.0000000  
 Cl 0.7181766 -2.6870716 2.2206824  
 Cl -1.7419916 -5.4757487 -0.0000000  
 Cl 3.9445321 -0.5080941 4.0996361  
 Cl 0.9862441 2.1048265 -2.6994953  
 Cl -2.2670464 2.4006297 -1.7023493  
 Cl 2.9338335 1.6702132 -0.0000000  
 Cl 0.9862441 2.1048265 2.6994953  
 Cl -0.0421488 -0.1086326 -0.0000000  
 Cl 3.9445321 -0.5080941 -4.0996361  
 Cl 3.5904842 -1.6566030 -0.0000000  
 Cl -2.2670464 2.4006297 1.7023493  
 Cl 0.7181766 -2.6870716 -2.2206824  
 Cl -2.8976203 -1.5888562 1.7567640  
 Cl -6.0978404 0.9571544 -0.0000000  
 Cl -2.8976203 -1.5888562 -1.7567640  
 Cl 0.4527612 5.4735416 -0.0000000  
 first transition state A-C  
 La 4.2652558 -0.0553833 -0.8188320  
 La 1.0300635 -2.7430861 0.3939741  
 La -3.1198346 -2.1927520 -0.1396273  
 La -3.0492087 1.9670927 -0.1023839  
 La 0.7571022 2.9799754 0.7903168  
 Cl -0.3507696 0.2452155 0.1190620  
 Cl 6.8036751 -0.5946083 -0.4400809  
 Cl 3.4569055 2.3543099 0.5337090  
 Cl -0.9514005 -3.1367502 -1.6356073  
 Cl 2.7654082 -2.2495731 -1.7828925  
 Cl 1.8817399 -5.0943133 1.1329828  
 Cl 2.8487045 -0.9998801 1.5941053  
 Cl -1.3806278 -2.8781279 1.9479576  
 Cl -4.0489852 -0.1065523 1.5309564  
 Cl -3.4430855 -0.0787402 -2.0102056  
 Cl -5.0652594 -3.9184192 -0.3649177  
 Cl -5.0710655 3.5866956 -0.4292581  
 Cl -1.6437878 2.8134867 2.2326028  
 Cl 1.2939461 5.3023554 1.8442747  
 Cl 3.9606049 1.2611708 -3.0774546  
 Cl -0.9393810 3.5378842 -1.3186816  
 second transition state A-C  
 La 2.1833877 1.2945341 -2.1040161  
 La 1.2191943 -2.8328049 0.4825686  
 La -2.9696882 -2.0720443 0.1679779  
 La -2.1943848 2.0290597 -0.6023800  
 La 1.5636419 1.4150070 2.2771050  
 Cl 0.0860834 0.0379138 0.0419403  
 Cl 2.3760342 3.8760801 -1.5767037  
 Cl 3.6227025 1.3683523 0.5218796  
 Cl -0.9249647 -3.3010715 -1.3473218  
 Cl 2.7406614 -1.6084443 -1.4967197  
 Cl 2.3575397 -5.1518489 0.8832930  
 Cl 2.0354453 -1.2945164 2.7786315  
 Cl -1.1597126 -2.8616807 2.1467498  
 Cl -3.2426851 0.3969479 1.5239285  
 Cl -3.3152037 -0.2397791 -1.9325117  
 Cl -5.1157168 -3.5512647 0.3494297

Cl -3.9149675 3.9548841 -0.9890897  
 Cl -0.5314400 3.1376531 1.4822024  
 Cl 2.1987729 2.4361254 4.5972845  
 Cl 3.4893770 1.0204657 -4.3531084  
 Cl -0.5040767 1.9464316 -2.8511397  
 transition state B-C  
 La 2.1407075 -1.8474170 -0.8665768  
 La 0.0269128 -0.0511232 3.1357987  
 La -2.5183934 -2.0154657 -0.3293054  
 La -2.0383518 1.7788801 -1.8058957  
 La 2.3976672 2.2285327 -0.3981232  
 Cl -0.1890615 0.1420910 0.0298852  
 Cl 4.1014389 0.0393315 -0.0150462  
 Cl 1.8389908 0.4602417 -2.6204030  
 Cl -1.9505918 -2.0720601 2.3849173  
 Cl 1.8182867 -2.0901677 1.8851208  
 Cl 0.5594861 -0.5230371 5.6646353  
 Cl 1.9324555 2.0190306 2.3331350  
 Cl -1.8459250 1.8159149 3.0325082  
 Cl -3.8235256 0.5559091 -0.0994684  
 Cl -2.0652952 -0.7264500 -2.9404102  
 Cl -4.4827847 -3.6936960 -0.6977996  
 Cl -3.4630302 3.2639945 -3.4079794  
 Cl 0.0140534 3.5976250 -1.2519245  
 Cl 4.0679663 4.1653601 -0.9133314  
 Cl 3.7177385 -3.6343777 -1.9379102  
 Cl -0.2387445 -3.4131167 -1.1818267

$\text{La}_6\text{Cl}_{19}^-$   
 isomer A  
 La 3.4080715 -0.0000000 -0.0000000  
 La 0.0000000 0.0000000 -3.4080715  
 La -0.0000000 -3.4080715 0.0000000  
 La 0.0000000 0.0000000 3.4080715  
 La 0.0000000 3.4080715 0.0000000  
 La -3.4080715 0.0000000 -0.0000000  
 Cl 0.0000000 -6.0085157 0.0000000  
 Cl -0.0000000 -2.7505257 -2.7505257  
 Cl 6.0085157 -0.0000000 -0.0000000  
 Cl 2.7505257 -2.7505257 0.0000000  
 Cl 2.7505257 -0.0000000 -2.7505257  
 Cl -0.0000000 -0.0000000 -6.0085157  
 Cl -2.7505257 2.7505257 0.0000000  
 Cl 2.7505257 2.7505257 0.0000000  
 Cl -0.0000000 -2.7505257 2.7505257  
 Cl -2.7505257 -2.7505257 0.0000000  
 Cl 0.0000000 6.0085157 0.0000000  
 Cl -2.7505257 0.0000000 2.7505257  
 Cl 0.0000000 0.0000000 0.0000000  
 Cl 0.0000000 2.7505257 2.7505257  
 Cl -6.0085157 0.0000000 -0.0000000  
 Cl -2.7505257 0.0000000 -2.7505257  
 Cl 0.0000000 2.7505257 -2.7505257  
 Cl 2.7505257 -0.0000000 2.7505257  
 Cl -0.0000000 -0.0000000 6.0085157  
 isomer B  
 La -1.4106269 -2.4432775 -2.0692995  
 La -1.3740710 2.3799607 2.1419358

La -1.3740710 -2.3799607 2.1419358  
 La -1.4106269 2.4432775 -2.0692995  
 La 2.7481420 0.0000000 2.1419358  
 La 2.8212538 0.0000000 -2.0692995  
 Cl -2.4609743 -4.2625326 -3.6041254  
 Cl -0.1302907 -3.8118691 0.0335069  
 Cl -3.2360302 2.0187696 0.0335069  
 Cl -2.2730208 0.0000000 -3.1998119  
 Cl -2.4388463 4.2242058 3.6427515  
 Cl 1.1583167 -2.0062633 3.3410323  
 Cl -3.2360302 -2.0187696 0.0335069  
 Cl -2.4388463 -4.2242058 3.6427515  
 Cl -2.4609743 4.2625326 -3.6041254  
 Cl 0.0000000 0.0000000 0.2071433  
 Cl -2.3166333 0.0000000 3.3410323  
 Cl -0.1302907 3.8118691 0.0335069  
 Cl 3.3663209 -1.7930995 0.0335069  
 Cl 3.3663209 1.7930995 0.0335069  
 Cl 1.1365104 -1.9684937 -3.1998119  
 Cl 4.9219487 0.0000000 -3.6041254  
 Cl 1.1365104 1.9684937 -3.1998119  
 Cl 4.8776927 0.0000000 3.6427515  
 Cl 1.1583167 2.0062633 3.3410323  
 isomer C  
 Cl -0.0395803 5.9748182 4.1481633  
 Cl -0.0873216 5.9340184 -3.4315175  
 Cl 0.0000000 0.0000000 -6.2667099  
 Cl 0.0873216 -5.9340184 -3.4315175  
 Cl 0.0395803 -5.9748182 4.1481633  
 La 0.0185317 4.0343448 2.3886289  
 La 0.0025873 3.9396288 -1.7458230  
 La 0.0000000 0.0000000 -3.6717778  
 La -0.0025873 -3.9396288 -1.7458230  
 La -0.0185317 -4.0343448 2.3886289  
 Cl -1.8038253 2.0039198 -2.8308350  
 Cl -0.2337892 -1.7056283 0.3480216  
 Cl -1.7547089 -4.8918089 0.3113998  
 Cl -1.7210973 -2.0247820 3.5551816  
 Cl -1.8248929 4.6605059 0.3239194  
 Cl 1.8248929 -4.6605059 0.3239194  
 Cl 1.8038253 -2.0039198 -2.8308350  
 Cl 0.2337892 1.7056283 0.3480216  
 Cl 1.7547089 4.8918089 0.3113998  
 Cl 1.7210973 2.0247820 3.5551816  
 Cl -1.8175415 2.0172133 3.3270825  
 La 0.0000000 0.0000000 2.5762514  
 Cl 1.8175415 -2.0172133 3.3270825  
 Cl -1.7884547 -2.0914662 -2.9904516  
 Cl 1.7884547 2.0914662 -2.9904516  
 transition state A-B  
 La 3.1863024 0.3265012 0.4413345  
 La -0.6473322 -0.1880422 -3.4521983  
 La 0.1908446 -3.3242946 -0.1425710  
 La -0.3142125 -0.6654760 3.9237471  
 La 0.6835622 3.3711843 -1.3081531  
 La -2.8086469 0.4314868 0.6204368  
 Cl 0.2001736 -5.9180547 -0.3910408  
 Cl 0.4631787 -2.6994728 -2.9238870

Cl	5.7810234	0.5402048	0.5221033
Cl	2.9031663	-2.4392839	-0.0344326
Cl	2.5475686	1.2799730	-2.2126406
Cl	-1.1363785	-0.7454340	-5.9416431
Cl	-1.9027146	3.0817079	-0.3988326
Cl	2.2958597	2.9832639	0.9428755
Cl	0.2589705	-3.1362578	2.6994469
Cl	-2.4439240	-2.4274336	-0.1769568
Cl	1.2128919	5.8631214	-1.8408072
Cl	-2.9122918	-1.1691156	3.0393458
Cl	0.1014670	-0.0625906	-0.3307401
Cl	-1.0756868	1.6754172	2.6498534
Cl	-5.2971007	1.1679396	0.8541202
Cl	-3.0923369	0.2321190	-2.3353602
Cl	-0.2357369	2.5486510	-3.8601867
Cl	2.3561631	-0.0632686	3.1192308
Cl	-0.3148104	-0.6628458	6.5369558

## References

- 1 J. P. Perdew, K. Burke and M. Ernzerhof, Generalized gradient approximation made simple, *Phys. Rev. Lett.*, 1996, **77**, 3865-3868.
- 2 J. M. Tao, J. P. Perdew, V. N. Staroverov and G. E. Scuseria, Climbing the density functional ladder: Nonempirical meta-generalized gradient approximation designed for molecules and solids, *Phys. Rev. Lett.*, 2003, **91**, 146401.
- 3 M. Lukanowski and F. Weigend, *manuscript in preparation*.
- 4 M. Dolg, H. Stoll, A. Savin and H. Preuss, Energy-adjusted pseudopotentials for the rare-earth elements, *Theor. Chim. Acta*, 1989, **75**, 173-194.
- 5 J. P. Perdew, M. Ernzerhof and K. Burke, Rationale for mixing exact exchange with density functional approximations, *J. Chem. Phys.*, 1996, **105**, 9982-9985.
- 6 Y. J. Franzke, N. Middendorf and F. Weigend, Efficient implementation of one- and two-component analytical energy gradients in exact two-component theory, *J. Chem. Phys.*, 2018, **148**, 10411.
- 7 Y. J. Franzke, L. Spiske, P. Pollak and F. Weigend, Segmented Contracted Error-Consistent Basis Sets of Quadruple- $\zeta$  Valence Quality for One- and Two-Component Relativistic All-Electron Calculations, *J. Chem. Theory Comput.*, 2020, **16**, 5658-5674.
- 8 D. Chai, M. Head-Gordon, Long-range corrected hybrid density functionals with damped atom–atom dispersion corrections, *Phys. Chem. Chem. Phys.* 2008, **10**, 6615–6620.
- 9 F. Weigend, M. Häser, RI-MP2: First derivatives and global consistency, *Theor. Chem. Acc.* 1997, **97**, 331-340.
- 10 Y. Zhao, D. G. Truhlar, *Theor. Chem. Acc.*, 2008, **120**, 215-241.
- 11 A. Arbuznikov, M. Kaupp, Towards improved local hybrid functionals by calibration of exchange-energy densities, *J. Chem. Phys.*, 2014, **141**, 204101.
- 12 O. Treutler and R. Ahlrichs, Efficient molecular numerical-integration schemes, *J. Chem. Phys.*, 1995, **102**, 346-354.